ESTIMATION OF OBJECTS SOLAR POTENTIAL USING LIDAR DATA

Niko LUKAČ, Danijel ŽLAUS, Natalija TRSTENJAK, Borut ŽALIK

ABSTRACT

Solar energy is an attractive resource to gain electrical energy. Although this resource is renewable and available every day, the maximum amount of incoming energy depends on various factors. In this paper, a method to calculate solar potential of the buildings roofs, for a given location and time frame is given. The proposed method considers position and orientation of Earth in respect to the Sun, inclination of objects and surfaces using detailed topography obtained from LiDAR, influence from shadowing and meteorological effects. The maximum solar energy is adjusted according to the shadowing and meteorological influence. In this way, proposed method gives a better approximation of the real world solar energy potential.

1. INTRODUCTION

It is possible to calculate the maximum theoretical solar radiation with good approximation on a given location and time frame, with the help of calculating the Earth's position and orientation in respect to the Sun. The calculated energy will never be the exact energy the solar power plants receive in practice, because the final received energy depends on many other factors, which include: geographical location of the solar power plants, local meteorological influence (e. g. temperature, air moisture and number of sun hours) and topography (surface inclination). Meteorological factors cannot be calculated and are gained from different measurements (from meteorological stations to meteorological satellites). Topographic data from the Earth's surface can be obtained from many sources: DEM (digital elevation model), aerial photographs and LiDAR (Light Detection And Ranging). With the use of the inclination information from the topography, it is possible to calculate the angles between the surface and the Sun's rays. These angles define the intensity of the received solar energy. LiDAR-based data is the main source to perform shadowing algorithms, because of the precise 3D available information for the objects and surface.

Estimation of solar potential has been done for a long time in field of geographical information systems (GIS) [2]. Many solutions use DEM-based topography data [1, 3, 4] in order to calculate the required inclinations and to perform shadowing. DEM-based topography gives low resolution information, therefore it is better to use classified LiDAR data [5, 6, 7, 8], especially as this enables more precise calculation of the shadows. Solutions [5, 6] also consider meteorological effects.

In this paper, a method to estimate solar potential for objects on a given location and a time frame is considered. Detailed topography of the Earth's surface and objects is obtained from classified LiDAR data. The maximal theoretical received solar energy is calculated and decreased depending on the shadows and meteorological influence.

The paper is organized into 5 sections, where section 2 briefly describes LiDAR technology and data classification. Section 3 describes the solution, while Section 4 gives experimental results of the proposed method. The conclusion describes the findings and gives hints for future improvements.

2. LIDAR DATA

Aerial laser scanning or LiDAR is a technology for remote sensing of Earth's surface and the objects on it. LiDAR is an active instrument that sends short laser pulses on a given surface and observes their reflection. It is possible to calculate the point positions, depending on the time and distance the laser pulse travels from the surface to the receiver. Besides from the position, LiDAR instrument also measures the angle, time and intensity of the reflection [9].

The sensor works in visible and infrared spectra (EMV wave length is between 800 - 1100 nm, frequency is between 5 - 200 kHz), where the reflection of vegetation is maximum and the potential of harming human vision is minimal. Accuracy of the data is dependant from the scanning parameters. To calculate solar potential, the estimated optimal point density is between 1 and 4 $points/m^2$, which assures optimal ratio between the data capacity (number of points) and their accuracy [10]. When scanning with this point density, the ensured positional accuracy is up to 0,25m and the height accuracy up to 0,15m, which is enough to obtain reliable level of results for a town or region.

The result is a 3D point cloud, written with geographic coordinates and many other attributes, which describe surface features. In order to interpret the data correctly, we filter them to remove unnecessary points. After filtering a DEM is obtained. Classification, known as recognition of geometrical structures or objects is the next important step. From the classification, a qualitative layers that arrange the points into one of the following classes is obtained:

- surface,
- objects: buildings and roofs,
- high vegetation: forest and isolated trees,
- other: low vegetation, automobiles…

Using the objects class it is possible to calculate solar potential for every building.

3. PROPOSED SOLUTION

Firstly, classified LiDAR data has to be prepared, where point cloud is inserted into an equally-sized grid. The size of a cell in the grid depends on the chosen resolution (e.g. $0{,}5\mathrm{m}^2$). The height of the cell is determined by the highest point that falls into it. In fig. 1 the difference can be seen in visualizing the raw LiDAR point cloud, and the processed point cloud on the grid.

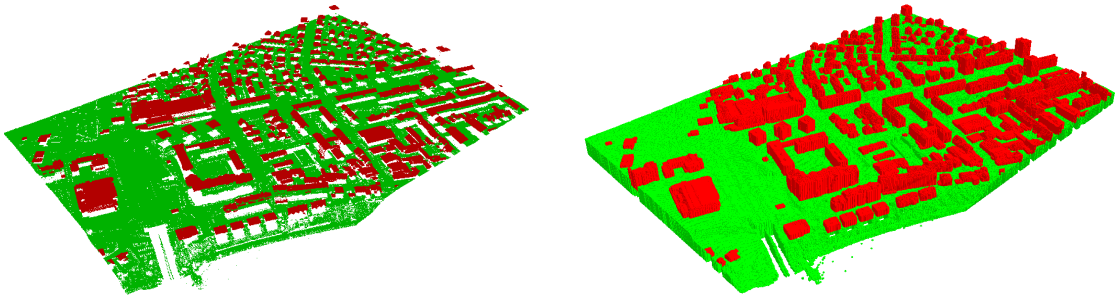

a) *b)*

Fig. 1: Visualizing LiDAR data using a) points and b) grid.

Using the grid, an average of received solar energy for a specific geographic location and time frame can be calculated. Various factors such as shadowing, meteorological influence, and the topography of the Earth's surface is taken into account. The most important factors are the geographic location and time frame, since the Earth's axis is tilted and its distance from the Sun varies [11]. As a consequence this affects the maximum solar energy of a cell $E_{max\ cell}$, which is calculated using the method described in [18].

3.1 Position of the Sun

In order to calculate the shadows on the surfaces, the position of the Sun is simulated. The simulation uses coordinated universal time (UTC) and position on Earth, which is obtained by averaging GPS data from the LiDAR point cloud. The Sun's position using the astronomical Almanac algorithm [13] has been approximately calculated. The simulated position is, on average, different by 0,1% compared to the real world data from the Griffin observatory [15]. In fig. 2 the resulting 3D graph represents the Sun's angle (azimuth) for the year 2010. The most visible characteristic is the shift to and from daylight time savings (DTS) in March and October. If we observe the edge of the graph, we can see when the Sun rises and sets throughout the year.

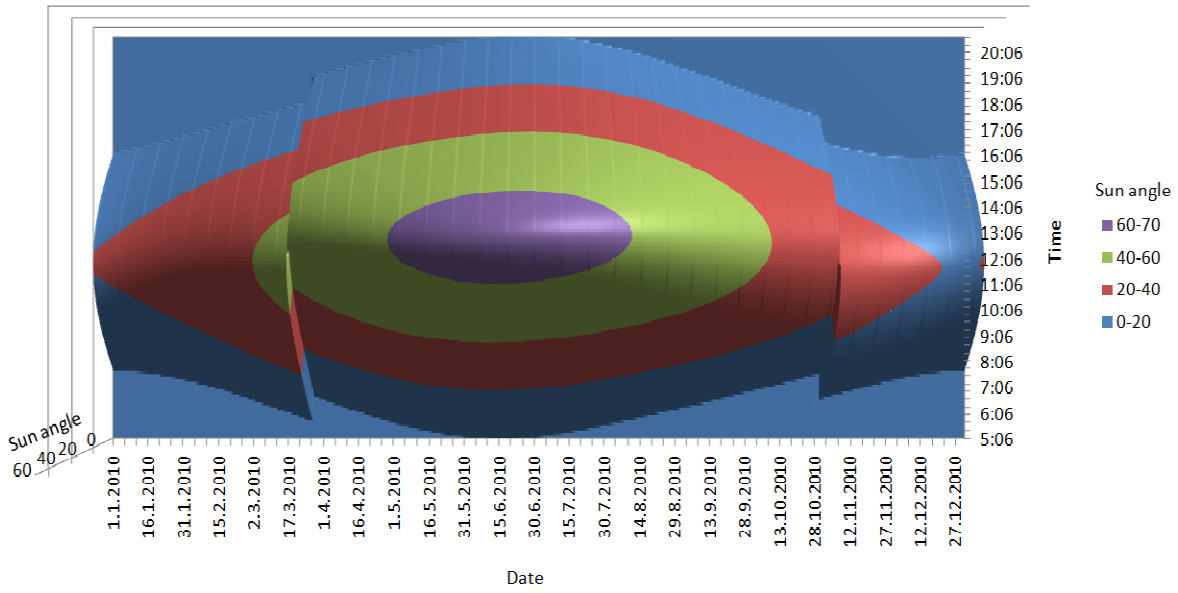

Fig. 2: The Suns angle throughout the year 2010.

3.2 Surface shadowing

With the simulation of shadows, the maximum solar energy is effectively reduced. When determining whether the roofs of buildings are shadowed, the following scenarios are considered:

- an non-flat roof can be in the shadows for a given time in a day,
- a roof can be shadowed by the surrounding terrain or neighbour buildings,
- chimneys and objects on the top of the roof can contribute to shadowing.

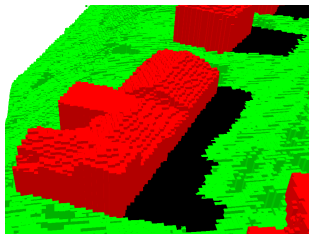

Fig. 3: A part of the terrain and buildings, where the shadows fall under the same angle.

The shadowing algorithm [16] is applied to the grid, generated from LiDAR data. The Sun's rays directional vector is extracted by subtracting the centre point of the grid from the Sun's position. It is assumed that the shadowed area is small enough, that the curvature of the Earth has a negligible influence. Consequently all the shadows have the same angle for the entire grid (see fig. 3). The result of the shadowing is the average of all the shadows that fell onto a cell, for a specific time frame. This information is then normalized into an interval $[0,1]$. In fig. 4 a part of Maribor can be seen with the average shadows in a 24 hour period

using time step of 1 hour, which spans between two days, for all four seasons in the year 2010.

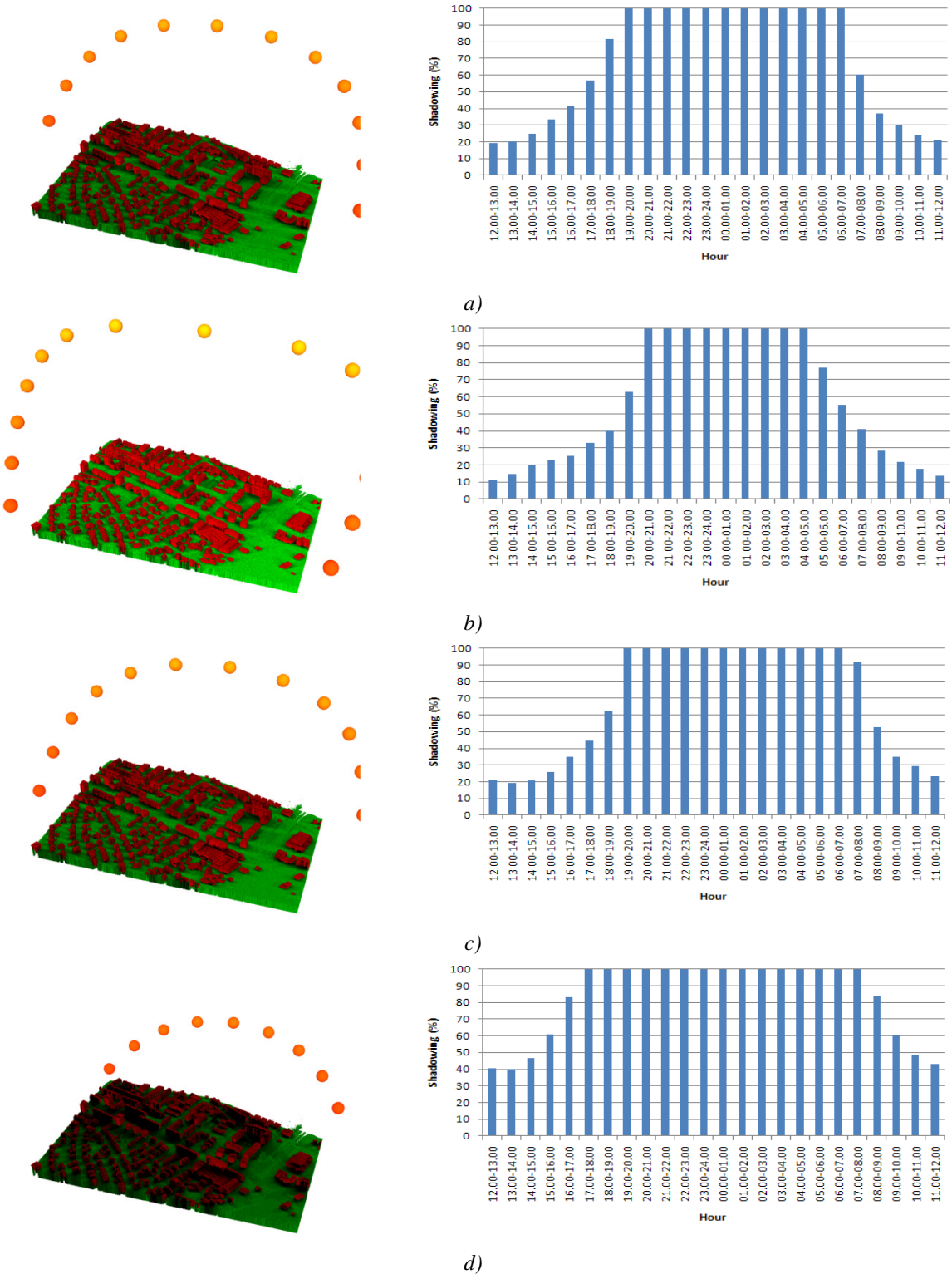

Fig. 4: Average shadows for a) 21-22.03.2010, b) 21-22.06.2010, c) 22-23.09.2010 in d) 21-22.12.2010

In fig. 4, the Sun's position for every hour in the day is also visualized.

3.3 Using meteorological data

With the described approach, the amount of solar insolation percentage (without shadowing) is determined. However, the simulation does not mirror real world conditions; therefore it is reasonable to take into the account meteorological influence for a specific time frame at a given location. This problem can be solved by using statistical data from weather stations in close proximity to a given location. For Slovenia, the data from ARSO [17] of the yearly average number of sun hours can be used. Depending on the time frame, we scale and normalize the solar hours into an interval $[0,1]$. It is known how much solar energy is, on average, reflected (~31%), i. e. albedo effect, and how much is absorbed (~20%) due to clouds [12], as can be seen in fig. 5.

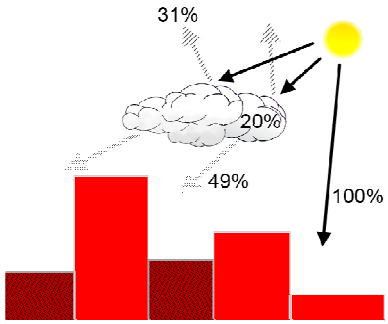

Fig. 5: An illustration of the clouds influence on solar insolation.

When the meteorological influence is taken into account, the obtained solar energy is determined as:

$$E_{cell_1} = \left(E_{max\_cell} - \left(E_{weather\_reflection} + E_{weather\_absorption}\right) * NS\right)\left[\frac{\mathrm{kWh}}{\mathrm{m}^2}\right] \quad (1)$$

where:

- E_{cell_1} - solar energy of the cell with included meteorological influences,
- $E_{max\ cell}$ - maximum solar energy of the cell,
- $E_{weather\_reflection}$ - 31% of $E_{max\ cell}$,
- $E_{weather\_absorption}$ - 20% of $E_{max\ cell}$,
- NS - percentage of hours without a clear sky $(1 - SunHours)$.

3.4 Calculation of the solar potential

The average solar potential for each cell has been calculated by taking into account the position, time, shadowing, meteorological influence, and topography. Distributing the solar potential is mainly dependant on the topography of the Earth's surface [14]. One topographic feature of a cell is its inclination expressed by its normal vector. Using the Sobel filter [19] the normal vectors over the entire grid of cells can be efficiently calculated.

The percentage of received solar energy on surface depends on the angle β between the normal vector of a cell and the Sun's rays vector (see fig. 6). The amount of the solar energy is then calculated as the function of $cos(\beta)$.

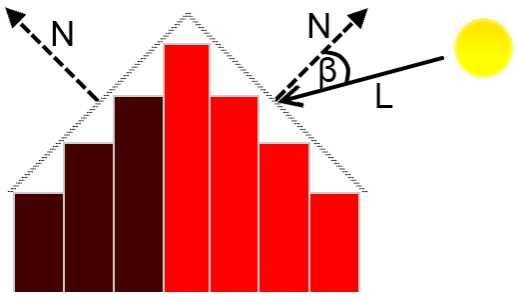

Fig. 6: An illustration of the normal vector *N*, the sunlight vector *L* and angle β.

The final equation for the average solar potential in our method is:

$$E_{cell} = \left(E_{cell_1} * (1 - shadowing) * cos(\beta)\right)\left[\frac{\text{kWh}}{\text{m}^2}\right] \quad (2)$$

where:

E_{cell}	- the average solar energy of the cell,
E_{cell_1}	- solar energy of the cell with included meteorological influences,
$shadowing$	- the percentage of shadowing of the specific cell,
β	- angle between the cell's normal vector and Sun's rays vector.

4. RESULTS

We implemented the described method in the programming language C++ and for visualization the OpenGL library has been used. The used hardware was: processor Intel Core 2 Duo (2,93Ghz), 4GB system memory and Ati Radeon HD4600 1GB graphical card. The method was tested on the classified LiDAR data for a part of Maribor (GK coordinates of the area: 548000, 158001, 548779, 158500), which stretches over an area of ~0,37km^2. The average solar potentials for all four seasons in year 2010 have been calculated, as shown in fig. 7. The solar potentials were calculated using a time step of 1 hour with the grid cell's resolution of $0{,}5\text{m}^2$.

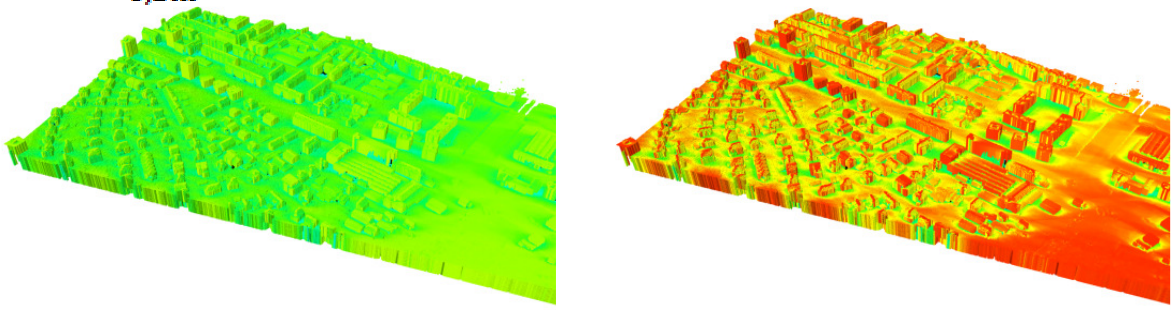

a) *b)*

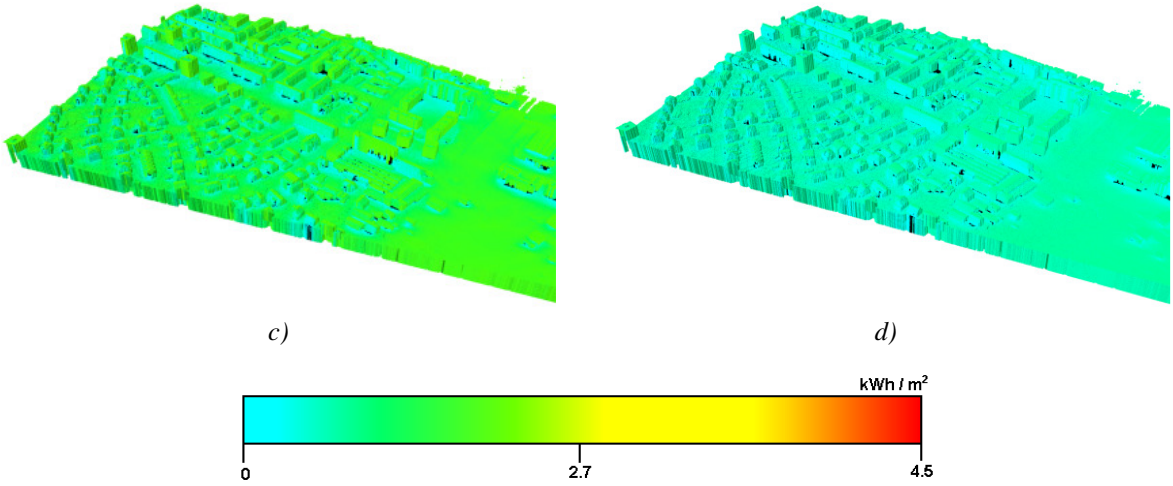

Fig. 7: Displaying the average calculated solar potentials for all four seasons a) 21.03-21.06.2010, b) 21.06-22.09.2010, c) 22.09-21.12.2010 and d) 21.12.2010-21.03.2011.

The average solar potential per hour for the year 2010 can be observed in fig. 8. The distribution is close to Gaussian with its peak in the summer.

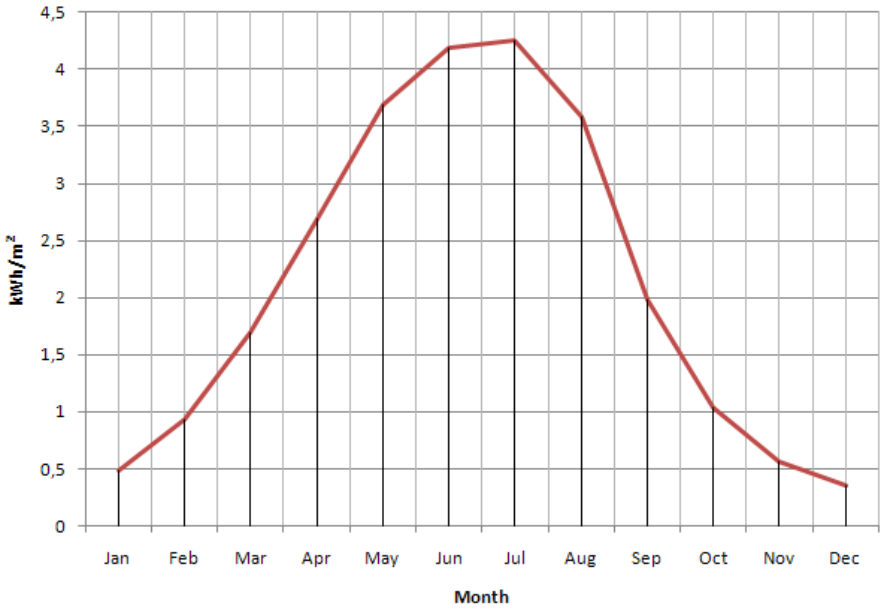

Fig. 8: Average solar potential of our tested area for each month in 2010.

The average solar potential per hour, for the year 2010, is shown in fig. 9. Flat surfaces have a higher solar potential, due to the angle between the surface and the Sun's rays. The solar potential for the buildings is shown in fig. 9b.

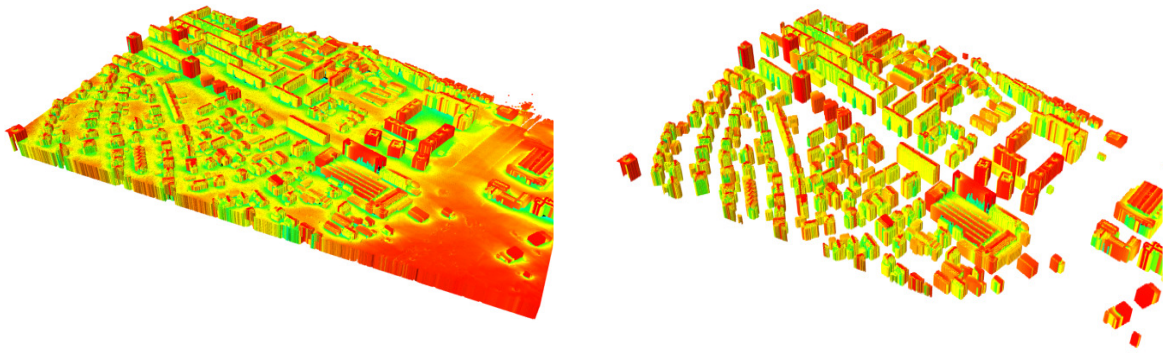

a) *b)*

Fig. 9: Displaying the average calculated solar potential for the year 2010 for the whole region (a) and only for buildings (b).

We measured the spent CPU time of our method (see table 1). For higher accuracy we repeated the measurements three times and averaged the final times.

Table 1: Measurements of spent CPU time of the proposed method.

	T. S.	**A. R.**	**T. S.**	**S. R.**	**T. S.**	**S. R.**
	1h	$1m^2$	0,5h	$1m^2$	1h	$0,5m^2$
Time frame	**Time to calculate [s]**					
21.03.2010 - 21.06.2010	164,5		331,3		1267,2	
21.06.2010 - 22.09.2010	165,8		332,8		1274,5	
22.09.2010 - 21.12.2010	122,8		237,6		867	
22.12.2010 - 21.01.2011	118,2		232,7		831	

Used abbreviations: time step (T. S.), spatial resolution (S.R.).

It can be seen in table 1 that the fastest calculations are done for the winter season, since nights are longer and consequentially buildings are longer in the shadows.

5. CONCLUSION

The proposed method gives a good approximation of the solar potential of one or multiple objects, for a given geographical location and time frame. The approximation of the calculation gets closer to real world conditions when the accuracy of LiDAR data and measurements of meteorological effects is increased. The calculations of the larger areas and longer time frames can be done in a preprocessing phase in order to allow instant look up of the results at later times (e.g. viewing from a web application). The method will be modified to support parallel processing and other factors (e.g. vegetation), which can increase the approximation closer to the real-world solar potential.

6. REFERENCES

[1] Xavier Ponsa, Miquel Ninyerolab, Mapping a topographic global solar radiation model implemented in a GIS and refined with ground data, International journal of climatology, vol. 28, pp. 1821-1834, 2008

[2] Hetrick, W.A., Rich, P.M., Barnes, F.J., Weiss S.B., GIS-based solar radiation flux models, American Society for Photogrammetry and Remote Sensing Technical Papers, GIS Photogrammetry and Modeling, vol. 3, pp. 132-143, 1993

[3] Lalit Kumer, Andrew K. Skidmore, Edmund Knowles, Modeling topographic variation in solar radiation in a GIS environment, International Journal of Geographic Information Science, vol. 11, pp. 475-497, 1997

[4] Pinde Fu, Paul M. Rich, A geometric solar radiation model with applications in agriculture and forestry, Computers and Electronics in Agriculture, vol. 37, is. 1-3, pp. 25-35, 2002

[5] Kassner R., Koppe W., Schuttenberg T., Bareth G., Analysis of the solar potential of roofs by using official lidar data, The international archives of the photogrammetry, remote sensing and spatial information sciences, vol. XXXVII, pp. 399–403, Beijing, China, 2008

[6] Jochem A., Höfle, B., Hollaus, M., Rutzinger M., Object detection in airborne LiDAR data for improved solar radiation modeling in urban areas, The International Archives of the Photogrammetry, Remote Sensing and Spatial Information Sciences, vol. XXXVIII, pp. 1-6, Paris, France, 2009

[7] Jochem A., Wichmann V., Höfle B, Large area point cloud based solar radiation modeling, Hamburger Beiträge zur Physischen Geographie und Landschaftsökologie, vol. 21, 2010

[8] Dorothea Ludwig, Sandra Lanig, Martina Klärle, Sun-area Towards Location-based Analysis For Solar Panels By High Resolution Remote Sensors, International Cartographic Conference, Santiago de Chile, November 15-21, 2009

[9] Maune, D. F., 2008, Aerial mapping and surveying. In Land development hand-book (3th edn), S.O. Dewberry and L.N. Rauenzahn (Eds), pp. 877{910 (New York, NY: McGraw-Hill Professional).

[10] Jie Shan, Charles K. Toth ed., Topographic Laser Ranging and Scanning: Principles and Processing, CRC Press, 2008

[11] Muhammad Iqbal, An introduction to solar radiation, Academic Press Inc, New York, 1983

[12] John M. Wallace, Peter V. Hobbs, Atmospheric Science: An introductory survey, Academic Press, New York, 1977

[13] Joseph J. Michalsky, The Astronomical Almanac's algorithm for approximate solar position (1950–2050), Solar Energy, vol. 40, iss. 3, pp. 227 – 235, 1988

[14] Ralph C. Tempsa, K. L. Coulsona, Solar radiation incident upon slopes of different orientations, Solar Energy, vol. 19, iss. 2, pp. 179 – 184, 1977

[15] Griffith Observatory, Sunrise and Sunset 2010, Online: http://www.griffithobs.org/skyfiles/skysunrise2010.htm (10.01.2011)

[16] Matthew Strahan , Real-Time Heightmap Self-Shadowing Using the Strider Technique, Online:http://www,gamedev,net/page/resources/_/reference/programming/sweet-snippets/real-time-heightmap-self-shadowing-using-the-strider-technique-r2125 (22.06.2004)
[17] Republic of Slovenia Agency for Environment – ARSO, Online: http://www.arso.si/
[18] Gregg A. Stickler, Solar Insolation, NASA Goddard Space Flight Center, Online: http://edmall.gsfc.nasa.gov/inv99Project.Site/Pages/solar.insolation.html (26.6.2000)
[19] Bernd Jähne, Digital Image Processing, Springer, 2002

AUTHORS CONTACTS

Niko Lukač (niko.lukac@uni-mb.si), B.Sc [1]
Danijel Žlaus (danijel.zlaus@uni-mb.si), B.Sc. [1]
Natalija Trstenjak (natalija.trstenjak@geoin.si), B.Sc. [2]
Borut Žalik (zalik@uni-mb.si), Ph.D. [1]

[1] University of Maribor,
Faculty of Electrical Engineering and Computer Science,
Laboratory for Geometric Modelling and Multimedia Algorithms,
Smetanova ulica 17,
SI-2000 Maribor, Slovenia.

[2] Goedetic engineering d.o.o. – GEOIN,
Gosposvetska cesta 29,
SI-2000 Maribor, Slovenia